C. R. Physique 3 (2002) 1375–1392

Physique appliquée/*Applied physics*

DOSSIER

MÉCANISMES PHYSIQUES DU NUAGE D'ORAGE ET DE L'ÉCLAIR
THE PHYSICS OF THUNDERCLOUD AND LIGHTNING DISCHARGE

Observations and modeling of lightning leaders

Philippe Lalande [a], Anne Bondiou-Clergerie [a], G. Bacchiega [b], I. Gallimberti [b]

[a] ONERA, 29, av. de la division Leclerc, 92332 Châtillon, France

[b] I.R.S. Srl, via Vigonovese 81, 35127 Padova, Italy

Note presented by Guy Laval.

Abstract The development of atmospheric lightning is initiated by a 'leader' phase during which ionized channels appear in virgin air. The use of rapid cameras, the measure of fields and currents associated with the discharge allow one to compare the propagation of laboratory leaders with those of natural or artificially triggered lightning. The corresponding physical processes can be analyzed with the help of models developed for laboratory leaders provided that the non linear effects due to the intense current circulation leading to lightning leader thermalization are taken into account. A self-coherent simulation of triggered lightning leaders for both polarities is presented is this paper. Furthermore, these models make it possible to define the 'stabilization field' concept, equal to the minimum ambient field allowing the stable progress of a leader from a ground structure, expressed as a height and curvature function of this structure. This concept can be validated through triggered lightning tests. Finally, the stabilization field analysis is completed by a simplified analytical model based upon an electrostatic approach of propagation equilibrium. ***To cite this article: P. Lalande et al., C. R. Physique 3 (2002) 1375–1392.***

lightning / modeling / discharge / arc

Observation et modélisation du leader de l'éclair

Résumé Le développement de l'éclair atmosphérique est initié par la phase de « leader » correspondant à la formation de canaux ionisés dans l'air vierge. L'utilisation de caméras rapides, la mesure de champs et de courant associés à la décharge permettent de comparer les caractéristiques de propagation des leaders de laboratoire et ceux de l'éclair naturel ou déclenché artificiellement. Les processus physiques mis en jeu peuvent être analysés grâce aux modèles développés dans le cas du leader de laboratoire si l'on tient compte des effets non-linéaires dus à la circulation de courants intenses, conduisant à la thermalisation du leader de foudre. Une simulation auto-cohérente des leaders de l'éclair déclenché dans les deux polarités est présentée dans cet article. Par ailleurs, ces modèles permettent de définir le concept de « champ de stabilisation », égal au champ ambiant minimum assurant le développement stable d'un leader depuis une structure au sol, exprimé en fonction de la hauteur et du rayon de courbure de cette structure. Ce concept peut être validé grâce aux expériences d'éclairs déclenchés. Enfin, l'analyse du champ de stabilisation est complétée par un modèle analytique simplifié basé sur une approche électrostatique de l'équilibre de propagation. ***Pour citer cet article : P. Lalande et al., C. R. Physique 3 (2002) 1375–1392.***

foudre / éclair / décharge / modélisation / arc

E-mail address: lalande@onera.fr (P. Lalande).

S1631-0705(02)01413-5/REV

1. Introduction

Modeling of the leader phase of a lightning flash is necessary to predict the physical thresholds for the occurrence of lightning strikes to aircraft or grounded structures. The aim of the models described in the present paper is to provide numerical tools to simulate the inception and development of a lightning leader from a conductive object. For this purpose, we have based our investigation of basic mechanisms on the studies of long sparks in laboratory [1–3] for which self-consistent models have been elaborated [4,5] and which are described in a companion paper in this same volume [6]. In Section 2 of the present paper, the main characteristics of positive and negative leaders in laboratory long sparks are compared with those of leaders in natural and triggered lightning flashes. It turns out that the main difference between leaders in long sparks and natural lightning is in the conditions for the stable propagation of the leader as function of the external ambient field: this appears to be related to the non-linear plasma processes that drive the channel conductivity (Section 3). On this basis, the self-consistent models developed for the simulation of laboratory long sparks have been adapted to the case of the rocket-triggered lightning (Section 3). Finally, based on the model results, we suggest a general concept for the stable propagation of long discharges (Section 4); this simple concept is analytically formulated and its practical applications is discussed in conclusion.

2. Comparison between leaders in laboratory long sparks and in lightning flashes

2.1. Main features of leaders in laboratory sparks and lightning flashes

Laboratory discharges in rod to plane gaps submitted to impulse voltages of various waveshapes were exhaustively studied by the 'Les Renardières' Group [1–3]. Based on the results of these investigations, ONERA and the University of Padova developed self-consistent models of both positive and negative leaders [4,5]. These models have been fully validated in laboratory experiments. In order to extend the use of these models to lightning leaders, the differences between the inception and propagation processes of leaders in laboratory discharges and lightning flashes have been investigated.

The positive discharge in laboratory long sparks develops in background electric fields in the range of 100–200 $\mathrm{kV{\cdot}m^{-1}}$. This discharge consists of two regions with different conductivity [6]: the corona front, which is a region of high resistivity where the ionization processes occur, and the leader channel, which is a conductive plasma channel from which the corona front develops. The potential gradient along the leader channel is of the order of 100 $\mathrm{kV{\cdot}m^{-1}}$. During the leader propagation, the two regions are strongly coupled. The leader head propagates continuously from the high voltage electrode to the ground plate, with a velocity from 10^4 $\mathrm{m{\cdot}s^{-1}}$ to 3×10^4 $\mathrm{m{\cdot}s^{-1}}$. The current flowing into the electrode is an almost continuous current of a few amperes. However, for slowly varying impulse fronts of the voltage (typically above 500 μs for a 10 m gap), discontinuities associated with sharp channel re-illuminations appear in the leader development [1,2,7]. When the corona front reaches the ground, an arc develops leading to complete breakdown of the air gap [7].

Berger [8] filmed at Mount San Salvatore the development of several upward positive lightning leaders from tall towers in ambient electrical fields of 10–50 $\mathrm{kV{\cdot}m^{-1}}$. Fig. 1(a) shows that the leader propagation is almost continuous (i.e., without steps), but it exhibits a discontinuous luminous emission with bright spikes about 25 μs apart. The two positive leaders in Fig. 1(b) are from two different towers; they propagate with velocities ranging from 2×10^4 $\mathrm{m{\cdot}s^{-1}}$ to 3×10^5 $\mathrm{m{\cdot}s^{-1}}$ (Fig. 1(b)). The current measured at ground is almost continuous and it increases with time from several tenths up to several hundreds of amperes.

The negative leader in laboratory develops in ambient electrical fields in the range of 200–300 $\mathrm{kV{\cdot}m^{-1}}$, almost double those needed for positive leaders. The propagation of negative leaders is discontinuous both in space and time, with several bright steps associated with current pulses of several hundred of amperes, and separated by time intervals between 10 to 20 μs [6]. A weakly luminous complex structure develops in periods between these steps. The elongation of the leader at each step is typically of 1 m and occurs with a mean velocity of 10^5 $\mathrm{m{\cdot}s^{-1}}$ to 5×10^5 $\mathrm{m{\cdot}s^{-1}}$.

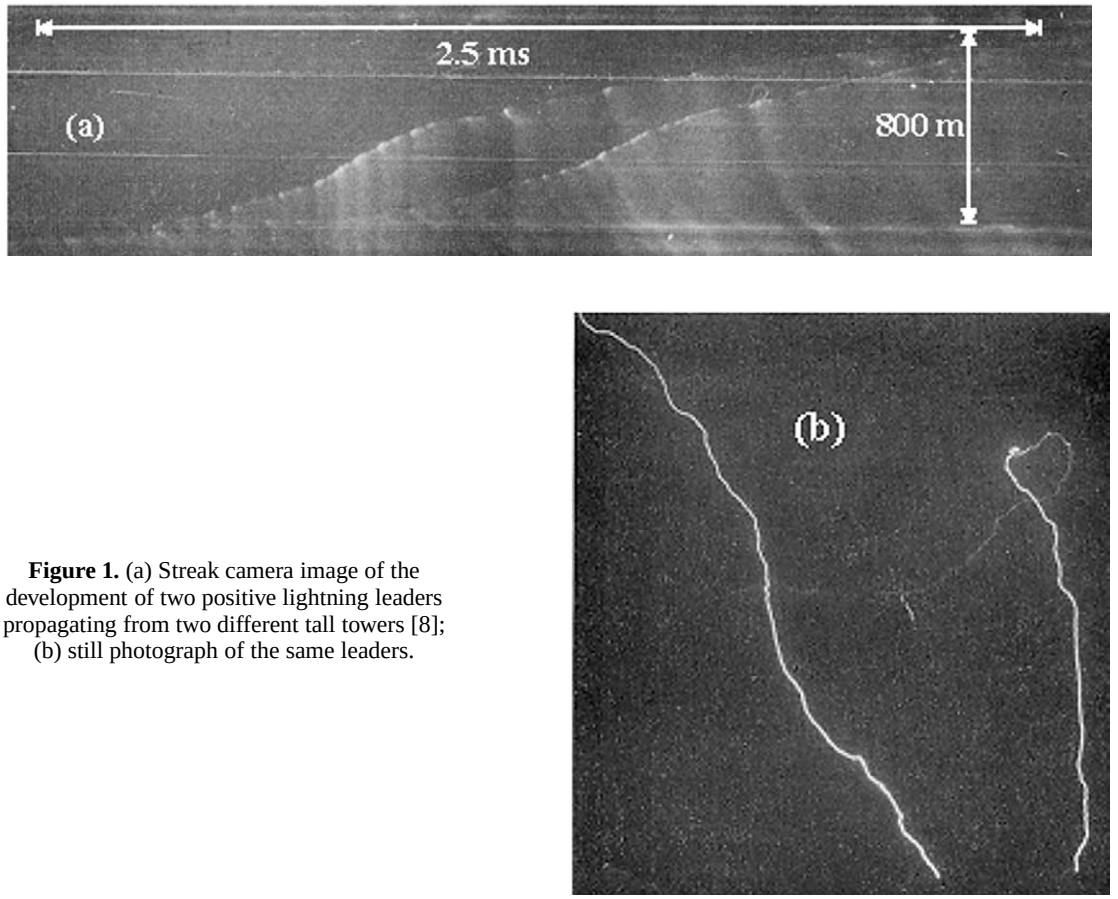

Figure 1. (a) Streak camera image of the development of two positive lightning leaders propagating from two different tall towers [8]; (b) still photograph of the same leaders.

Berger [8] also filmed a lightning upward negative leader from the top of a tall structure, in an ambient field greater than 40 kV·m^{-1} (Fig. 2). Its propagation is similar to that observed in laboratory, composed by bright steps of several meters; its mean velocity is in the range of 10^5 m·s^{-1} to 10^6 m·s^{-1}. The time interval between steps is approximately 30 µs. Currents measurements of negative leaders during the lightning strikes to aircraft show the peak currents associated with each step to be approximately 1 kA [9].

2.2. Features of leaders in rocket-triggered lightning flashes

Artificially triggered cloud-to-ground flashes can be obtained by a rocket spooling out a grounded wire in the ambient electric field E_0 produced by a thundercloud (so-called classic triggering technique) [10, 11]; such a flash is initiated by an upward leader from the rocket tip; in most cases, due to the polarity of the cloud charge, this is a positive upward leader. The leader characteristics are determined through the measurement of the current at the bottom of the wire and from fast cameragrams in streak mode.

These measurements have indicated that the artificially triggered positive leader exhibits the same discontinuous propagation as the natural one. Furthermore, it has been shown, from the analysis of the current traces, that the leader initiation process evolves in successive stages during the rocket ascent. At low altitude of the rocket, only aborted leaders develop; the current measurements show isolated groups of one or several pulses lasting from 5 to 20 ms (Fig. 3), followed by complete discharge arrest. The interval between successive pulses within each group is approximately from 20 to 30 µs.

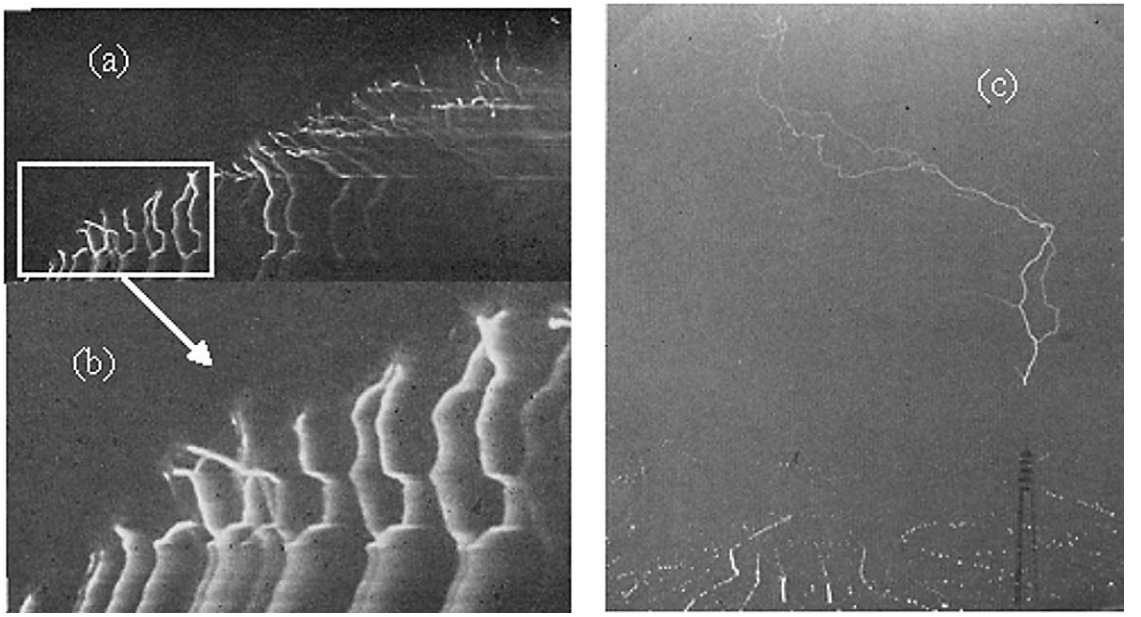

Figure 2. Development of an upward negative leader from a tall tower. (a) Streak camera image of the negative leader development; (b) zoom of a part of the streak camera image; (c) still photograph of the same lightning leader [8].

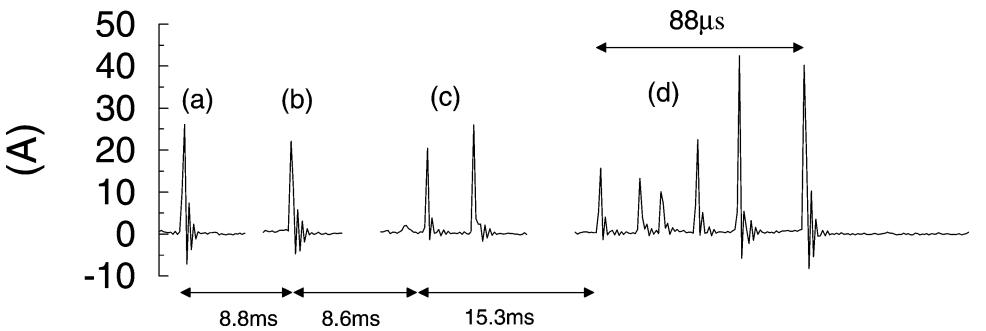

Figure 3. (a)–(c) and (d) groups composed of one (a), (b) or several (c), (d) oscillating current pulses associated with the attempted inception of upward positive leader in classical rocket-triggered lightning.

Each group of current pulses can be attributed to an attempted leader development and its extinction after a few meters, due to insufficient electric field above the rocket tip. The space charge injected by the discharge itself reduces the local electric field above the rocket tip and inhibits further development of the leader. Several milliseconds later, after the rocket has traveled a few meters through the space charge, the screening effect on the resulting field is reduced and a subsequent leader is then able to start.

At higher altitude, the onset of 'stable' leader propagation is observed: Fig. 4 shows the appearance at around 0.1 ms of a growing continuous current with superimposed pulses that are gradually damped. The continuous component may reach 200 A after tens of milliseconds. We believe that the pulses of the leader current are progressively filtered because of the relatively high resistance of the elongating leader channel in comparison with the wire resistance. The critical wire length for a stable leader propagation depends on the ambient electric field below the thundercloud.

In so-called 'altitude triggered' lightning (a variant of the classic technique), the rocket first spools out 50 m of grounded wire, followed by 400 m of insulating Kevlar thread (Fig. 5); finally, a second portion of the conducting wire is spooled. Bi-directional leaders initiate from the extremities of this floating wire, when it becomes sufficiently long [12]. A positive leader starts at the top of the rocket and propagates towards the cloud. A few milliseconds later, a downward negative leader starts at the bottom end of the triggering wire and propagates towards the ground. The whole process consists of the simultaneous propagation of two leaders of opposite polarities and is called 'bi-leader' or 'bipolar leader'. When the downward negative leader approaches the ground, an upward connecting positive leader starts from the upper end of the grounded wire followed by their connection and the subsequent arc.

The main features of positive and negative leaders originated from the floating wire have been inferred from cameragrams and electric field measurements on the ground [13]. As expected, the positive upward leader is similar to that generated with the classic triggering technique. Its propagation velocity ranges from 10^4 to 10^5 m·s^{-1}. Several aborted negative downward leaders are observed, through E-field variations,

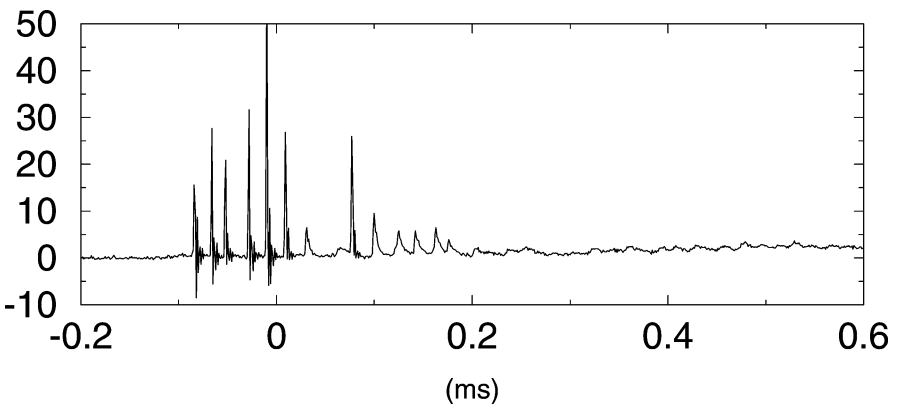

Figure 4. Current of an ascending positive leader in classical rocket-triggered lightning, measured on the ground.

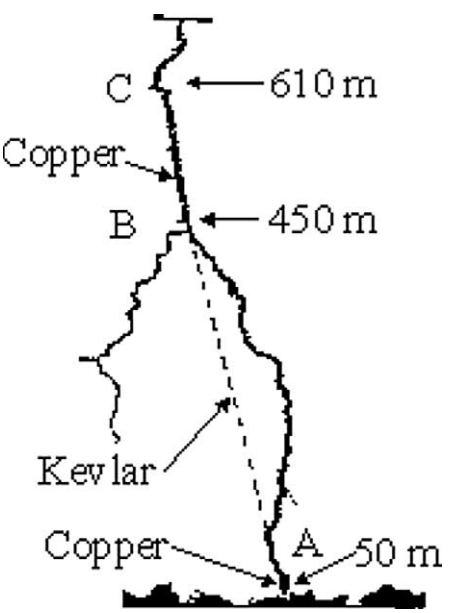

Figure 5. Photograph of an altitude triggered flash (summer 1989). The points A, B, C delimited the parts of the wire.

before a stable negative leader inception can take place. The propagation velocity of the negative leader is between 1 and 2×10^5 m·s^{-1}, with a stepping interval of 18–20 μs and a step length between 3 and 5 meters. E-field measurements indicate that each step transfers a charge of about 270 μC.

An acceleration of the upper positive leader is observed at the inception time of the negative leader at the bottom end; it indicates a coupling process between the two leaders, most likely through the potential variations of the floating wire. A similar coupling effect has been observed in laboratory bipolar leaders developing from a floating conductor positioned in the middle of a 10 m gap [14].

The propagation mode of rocket-triggered leaders is similar to that of laboratory leaders. However, the ratio between velocities and currents of lightning and laboratory are of the order of ten for both polarities. Furthermore, the lightning leaders can develop in ambient electric fields ten times lower than those for laboratory leaders. We shall show in the following section that the difference in leader currents leads to widely different internal fields in the channel (normal or thermalized leader channel [6]), and, therefore, to different conditions for a sustainable propagation.

3. Modeling of lightning leaders

3.1. Modeling of the leader channel: effect of the internal electric field

3.1.1. *Ambient and internal fields for leader propagation*

Let us consider the configuration of a grounded vertical wire of length Z_s in a uniform background field E_0 from which a leader develops to the height Z_a (Fig. 6). For simplification, we represent the leader as a channel with an internal electric field $E_i > E_0$ and neglect the corona region in front of it. The potential difference at the leader tip available to sustain the propagation is $\Delta V(Z_a)$. In laboratory, the internal field along the leader E_i is typically higher than 100 kV·m^{-1} for a positive leader [6]. The ambient field E_0 near the ground in thunderstorms, is usually in the range of 10 to 50 kV·m^{-1}. When the internal field E_i is higher than E_0, the potential difference $\Delta V(Z_a)$ decreases with the altitude Z; at the altitude Z_f, where it reaches zero, the leader development stops. Thus, a lightning leader can only develop if its internal electric field E_i becomes lower than the ambient electric field E_0.

3.1.2. *Evolution of the internal field versus current*

Experimental and theoretical analysis have shown that characteristics of the leader depends mainly on its current and charge (see [6]). In laboratory conditions, the current is relatively low, and ionization of neutral molecules is determined by electron-neutrals collisions; in this case, the temperature of neutrals

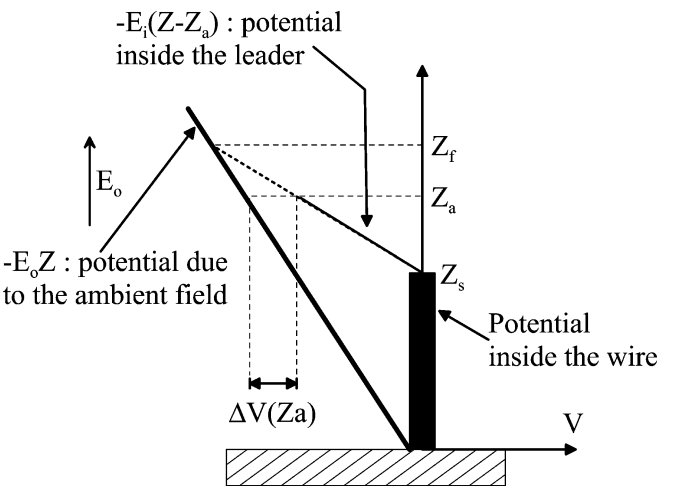

Figure 6. Potential distribution along the discharge propagation axis in the case of an ambient electric field E_0 lower than the internal electric field E_i.

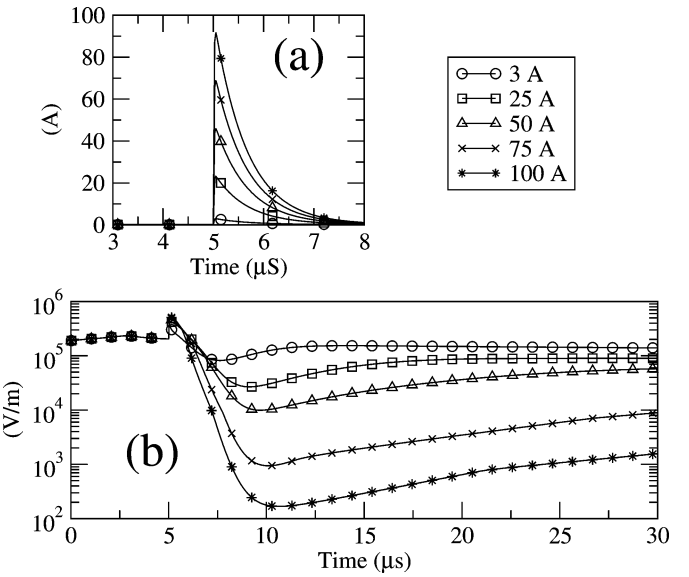

Figure 7. (b) Evolution of the leader internal field E_i for different values of the peak pulse current (a). The current pulse is injected at 5 μs.

remains in the range 4000–5000 K, far from local thermodynamic equilibrium (LTE); the electric field in the leader channel then maintains at relatively high values (above 100 kV·m^{-1}) which are characteristic of the 'normal' leader phase [6].

On the contrary for high current phases (final breakdown), the temperature raises above 5000–6000 K and the local thermodynamic equilibrium is obtained; the gas molecules are fully dissociated, the neutral, ion and electron temperatures become equal, and the ionization is determined by neutral-neutral collisions [6].

The lightning leader may be considered to be in a transition stage when a 'normal' leader channel transforms into a 'thermalized' channel, similar to the transition taking place just before the final arc in laboratory discharges. In this case, the gas temperature reaches values large enough for the ionisation to be dominated by thermal collisions [9].

The model presented in the companion paper [6] makes possible to calculate the temporal evolutions of densities, temperatures, channel radius, pressure and electric field as functions of current amplitude. In Fig. 7(a), the results obtained with pulses superimposed on a low continuous current of 0.2 A are presented; the peak currents (3, 25, 50, 75 and 100 A) are consistent with those measured in negative laboratory leaders and in lightning leaders of both polarities. The computer simulation shows that for current pulses lower than a few tens of amperes, the leader channel do not thermalized and its internal field remains of the order of 100 kV·m^{-1}. On the other hand, for larger current pulses (lightning leaders or strong negative laboratory leaders), the channel becomes thermalized and the internal field decreases down to 1–10 kV·m^{-1}, even if it increases slowly because of the cooling processes. Thus, due to the thermalization process and the low internal field, the lightning leaders can develop in low ambient electric field.

3.2. General principles for modeling of leader propagation

The numerical simulation of lightning leaders presented here is based on the self consistent time-dependent models described in the companion paper [6]. The input data is the initial field distribution (thundercloud electric field distorted by the rocket and wire); the different phases of leader inception and development are numerically simulated sequentially along the line of maximum electric field. The field and potential distributions are calculated by using a numerical method derived from the classical 'Charge Simulation Method' [15], taking into account the components of the leader channels and corona space charges. The inception and propagation parameters of the discharge (inception time, charge, current,

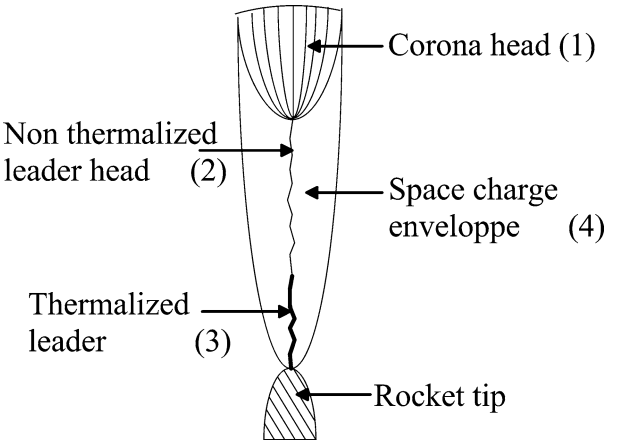

Figure 8. Representation of the regions of the positive leader. (1) Corona head where ionization and electron multiplication processes take place. (2) Leader channel: thin, medium temperature (1500 to 5000 K) conductive plasma channel ($E_{\text{int}} \approx 1$ kV·cm^{-1}); the current produced within the corona region feeds the leader progression and leader advancement sustains the E-field at the corona front. (3) Partly thermalized leader channel ($T > 5000$ K): increase of conductivity; $E_{\text{int}} \approx 10$ to 100 V·cm^{-1}. (4) Space charge envelope made of remnants of the corona head after propagation through it by the leader.

propagation velocity, conductivity, etc.) are derived for the different regions of the discharge (Fig. 8), as function of the local electric field distribution. The main steps of the simulation of a single leader are given in the flow chart in Appendix A.

3.3. Positive leader

The self-consistent model described above has been applied to the simulation of the inception and development of a positive leader in a 'classical' rocket triggered lightning, for different rocket altitudes. The results reported in this paragraph have been computed for a uniform ambient field E_0 of 40 kV·m^{-1} and two altitudes of the rocket tip, H: 50 m and 100 m. Figs. 9(a) and 10(a) show the temporal evolution of the vertical positions of the corona front and of the leader tip, for $H = 50$ m and 100 m, respectively. In agreement with experimental observations, the model shows that the upward leader propagation consists of a sequence of steps and restrikes, with a time interval between them of about 20 μs. Each step consists of the fast corona development, followed by the slow continuous propagation of the leader-corona system. The current at the leader tip (Figs. 9(c) and 10(c)) consists of a sharp pulse (associated with the fast corona development) and of a small continuous current (associated with the leader-corona propagation). The current records calculated from the model (Figs. 9(c) and 10(c)) are in good agreement with the current measurements at the bottom of the wire (Figs. 3 and 4) for an upward leader in classical triggered lightning.

For rocket height $H = 50$ m, the leader stops after a few steps with an elongation of about 12 m because the electric field at the leader tip becomes two low to sustain the corona development (Fig. 9(b)). In this case, the electric field at the leader tip is strongly reduced by the space charge accumulated during the first restrikes. However, with the rocket at $H = 100$ m, the discharge becomes stable and propagates without interruption because the electric field at the leader tip is always high enough for the development of a new corona at each restrike (Fig. 10(b)). As experimentally observed, an unstable propagation condition occurs at low altitude when the space charge effect grows faster than the leader extension effect (enhancement of the E-field at the tip); on the contrary, a sustained propagation can be obtained at higher altitude when the increase of the E-field at the leader tip due to the leader extension is high enough to counterbalance the effect of the space charge growth.

3.4. Bipolar leader

As in the previous case, the input data for the simulation of the bipolar leader development, in altitude triggered discharges, are the atmospheric electric field profiles (deduced form theoretical and experimental analysis) and the geometry of the rocket and wire system. The altitude-time development of both upward

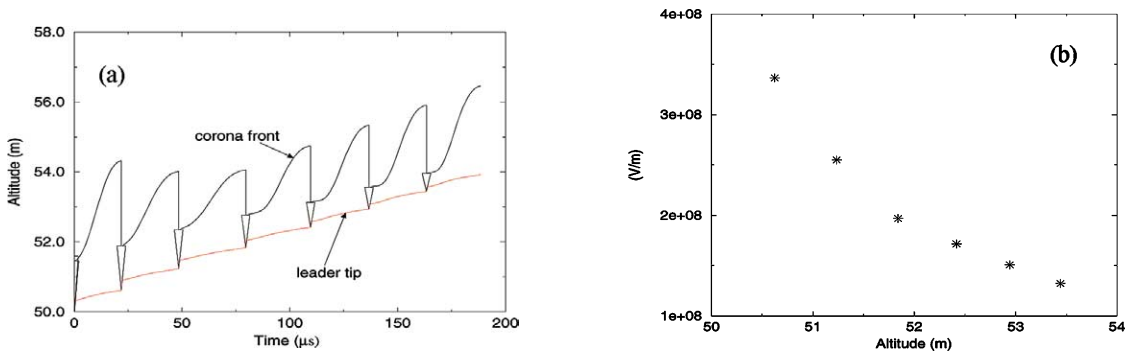

Figure 9. Model outputs for a rocket altitude $H = 50$ m. Calculated positions of the corona and leader heads (4a), temporal evolution of the electric field at the leader tip (4b), and the leader current (4c).

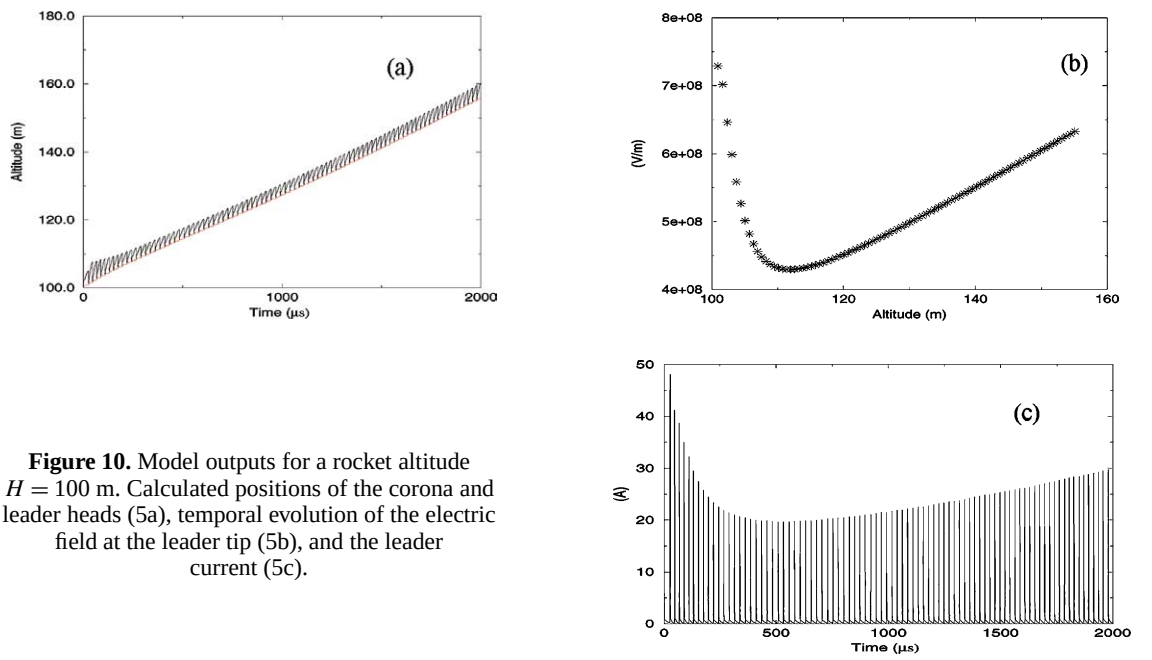

Figure 10. Model outputs for a rocket altitude $H = 100$ m. Calculated positions of the corona and leader heads (5a), temporal evolution of the electric field at the leader tip (5b), and the leader current (5c).

positive and negative downward leaders is shown in Fig. 11, with the main results of the simulation in Table 1.

The simulation results are mostly in good agreement with the measurement although several discrepancies can be emphasized. The length of the spooled wire at the positive leader onset is 160 m in the simulation

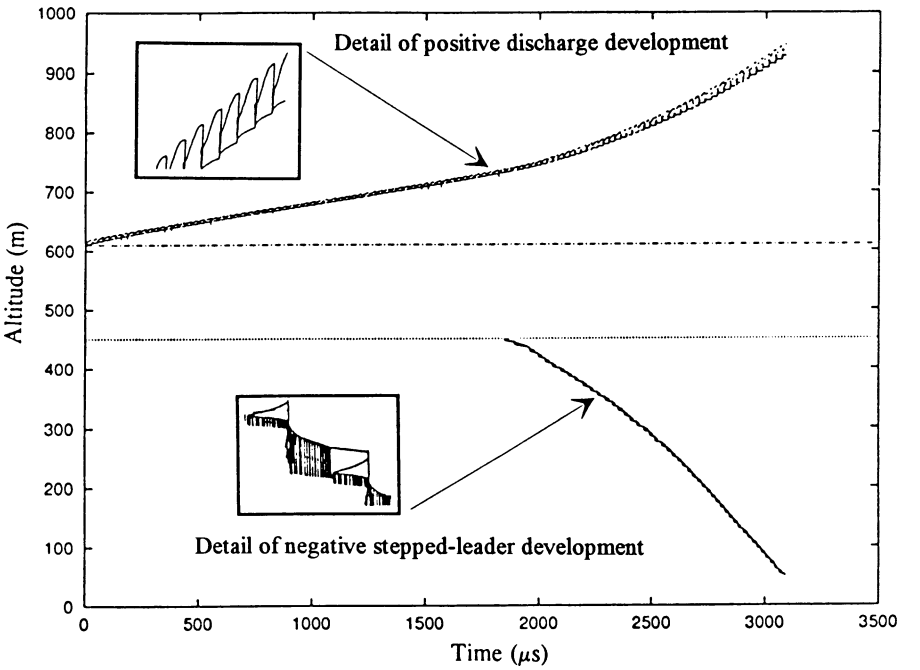

Figure 11. Simulated space-time development of the bi-directional leader in altitude triggered lightning. Calculation has been performed with a simplified electric field profile under a thundercloud inferred by the linear interpolation between the following points: 5.5 $kV{\cdot}m^{-1}$ (ground level), 60 $kV{\cdot}m^{-1}$ (at altitude of 400 m), and 70 $kV{\cdot}m^{-1}$ (at altitude of 600 m).

Table 1. Comparison between the calculated and measured parameters for the bipolar leader in an altitude triggered lightning experiment.

	Calculation	Measurements
Altitude of positive leader inception	610 m	560 m
Positive leader: δt between restrikes	28 μs	
Positive leader velocity	5×10^4–2.1×10^5 $m{\cdot}s^{-1}$	
Positive leader charge per unit length	65 $\mu C{\cdot}m^{-1}$	
Inception delay for the negative discharge versus the positive one	1.8 ms	3 ms
Negative leader stepping period	20 μs	18.5 μs
Negative leader step length	5–8m	<10 m
Negative leader velocity	2×10^5–4.5×10^5 $m{\cdot}s^{-1}$	4×10^5 $m{\cdot}s^{-1}$
Negative leader charge per unit length	110 $\mu C{\cdot}m^{-1}$	
Average E-field change associated with a step (at 50 m from the bottom of the wire)	35 $V{\cdot}m^{-1}$	25 $V{\cdot}m^{-1}$

versus 200 m measured. This discrepancy can be attributed to the fact that the simulation was performed with an approximate electric field profile. The time of the negative leader onset (1.8 ms for the simulation and 3 ms measured). This discrepancy is due to the fact that in our simulation (i) we have overestimated the

atmospheric electric field profile, and (ii) we did not take into account the effect of the negative space charge surrounding the bottom of the wire. The aborted negative leader generates this negative space charge, which reduces the electric field at the bottom of the wire and delays the onset of the downward negative leader.

4. Application of the physical discharge models to the concept of the stabilization field

4.1. Definition

For lightning protection purposes, it is necessary to evaluate the conditions leading to the formation and sustained propagation of a lightning leader from a grounded structure or a flying aircraft. The threshold condition is often estimated by a simple corona inception criterion. However, experimental observations of triggered lightning have shown that additional conditions must be fulfilled before a lightning leader can propagate over long distances. In these experiments (see previous sections), aborted leaders have been observed to propagate over a few meters and then stop if the average electric field in the discharge region is not sufficient to sustain their propagation.

From the physical models of both positive and negative discharges, a macroscopic criterion called the 'stabilization field' could be derived to represent the minimum threshold condition for the sustained propagation of a lightning leader from a grounded structure. For a thin cylindrical structure of height H, it is defined as the minimum uniform vertical atmospheric field that allows the stable propagation of an upward leader. This stabilization field can be derived from the self-consistent models described previously. Let us notice that we should normally add to this criteria and for ground structure, an accelerating electric field because the ground structure is usually surrounded by a space charge which tends to screen the atmospheric field. But as soon as an electric field instability occurs such as the approach of an downward leader or a strong wind which blows the space charge, an upward lightning leader will develop.

4.2. Derivation of the stabilization field from lightning leader models

For a 1 cm radius cylindrical rod of height H, terminated by an hemispherical tip, the 'stabilization field', $E_{\mathrm{stab}}(H)$, has been computed by using both positive and negative discharge models using a bisection method [16] on the values of atmospheric field E_0. The computation has been performed for different altitudes above the sea level and corresponding air pressures and densities.

The computed values of the stabilization field at sea level are plotted in Fig. 12 as a function of H for both positive and negative lightning leaders. For positive leaders from structures taller than 100 m, E_{stab} becomes lower than 30 kV·m^{-1}, the ambient field values frequently measured below a thundercloud. The model predicts that tall structures are likely to trigger cloud to ground flashes, initiated by a positive upward leader, as actually observed by numerous authors [17]. For a given structure height, the stabilization field of the negative discharge is two to three time larger than the one for the positive leader. This explains why in the bi-directional leader, the positive leader develops first and is following several milliseconds later by the negative leader onset. The positive leader development increases the floating potential of the suspended wire until it reaches the inception threshold of the negative lightning leader.

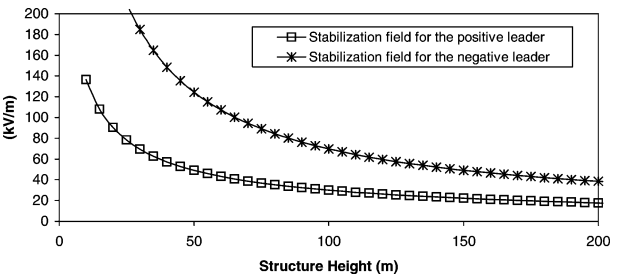

Figure 12. Stabilization field of a lightning leader as a function of the ground structure height.

Analytical formulas (1) and (2) have been derived from the numerical results by using a non-linear curve fitting method. They express the stabilization field as a function of the structure height, from a few meters to 400 m, and air density

$$E_{\mathrm{Stab}+}(H) = \left[\frac{306.7}{1+H/6.1} + \frac{21.6}{1+H/132.7}\right]\delta, \tag{1}$$

$$E_{\mathrm{Stab}-}(H) = \left[\frac{723}{1+H/10} + 4\right]\delta. \tag{2}$$

The stabilization field is in $\mathrm{kV\cdot m^{-1}}$ and the height is in meters. $\delta = (P/P_0)(T_0/T)$ where P and T, P_0 and T_0 are the ambient air pressure and temperature and the standard pressure and temperature at Mean Sea Level, respectively.

To compute the field threshold for the development of lightning leader from a ground structure with a height H and built at an altitude Z, you have just to compute the air density δ associated with this altitude and reported the height H and δ in the former expressions.

4.3. Validation of the modeling results for the case of the positive lightning leader

Using a small ascending rocket with an electric field sensor, launched immediately before the triggering rocket itself, Willett et al. [18] have measured the electrical ambient field profile just before a classical triggered lightning flash. They also measure the critical wire length H_T spooled out by the rocket when the flash occurs. They plot the mean ambient electric field E_{mean} along the rocket trajectory ($E_{\mathrm{mean}} = (1/H_T)\int_0^{H_T} E_0(z)\,\mathrm{d}z$) as a function of the length H_T (Fig. 13). The calculated values of the stabilization field versus the conductor height have been also plotted in Fig. 13. It turns out that the stabilization field is equal or slightly below E_{mean}. The small difference of few $\mathrm{kV\cdot m^{-1}}$ can be explained mainly by the fact that the distortion of the electric field distribution by the presence of previously aborted leaders has never been taking into account in the simulation. The reasonably good agreement between the simulation results and the measurements validates the stabilization field concept and allows us to use it as a quantitative tool for the design of ground or aircraft lightning protection [19].

4.4. Simplified electrostatic approach

Our self-consistent model of leader development is time dependent, i.e., all discharge parameters (charge, space charge radius, leader velocity, leader internal field, ...) are non-linearly coupled. In order to study independently the influence of each discharge parameter, we developed a simplified electrostatic model derived from the electrostatic modeling used in the self consistent model.

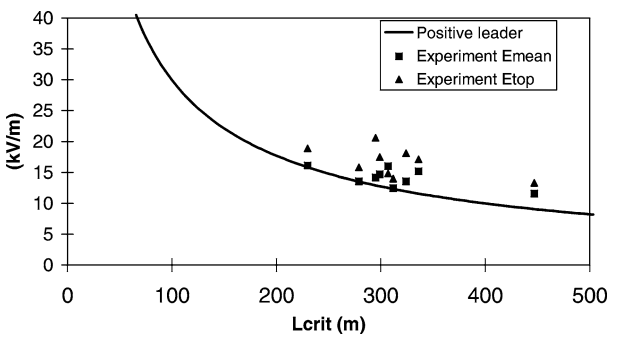

Figure 13. Comparison between the computed stabilization field of a positive lightning leader and the mean ambient field E_{mean} (mean value of the ambient electric field along the rocket trajectory) just before the lightning is triggered. E_{top} is the atmospheric electric field at the altitude of the rocket tip.

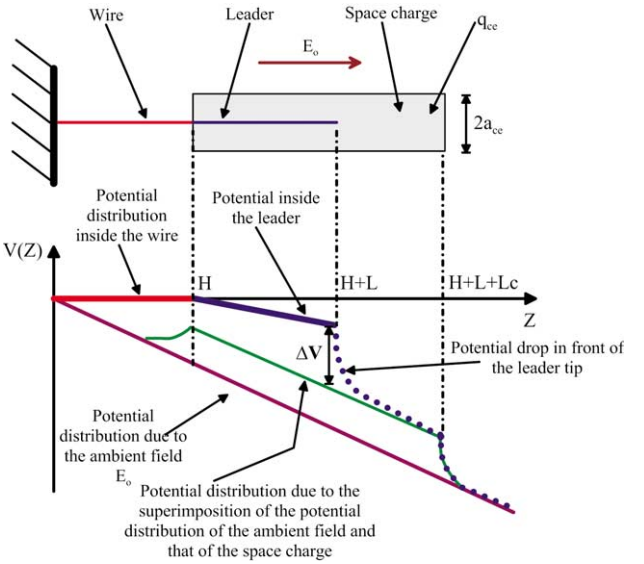

Figure 14. Scheme of the potential distribution along the leader propagation axis.

4.4.1. *Principle of the electrostatic model*

The configuration modeled is a grounded wire of length H from which a leader develops in a uniform ambient field E_0. A conductive leader channel is surrounded by a cylindrical space charge of radius a_{ce} and of uniform linear charge density q_{ce} (C·m^{-1}) (Fig. 14). The total space charge generated in the cylinder by the leader of length L is $q_{ce}L$. The leader internal field E_i is also assumed to be uniform.

At time t, when the leader has extended from H to $H + L$, the space charge envelope extends from H to $H + L + L_c$ where L_c is the length of the corona region in front of the leader head. The potential along the wire is constant and equal to zero, while, the potential along the leader channel is assumed to decrease with a constant slope E_i. The potential decreases sharply in front of the leader head to reach, a few meters away, the ambient potential.

The potential difference available to sustain the leader propagation is a function of the potential drop ΔV given by the following expression:

$$\Delta V = \Delta V_{am} - \Delta V_{le} - \Delta V_{ce}. \tag{3}$$

Here ΔV_{am} is the potential drop produced by the atmospheric field between ground and $z = H + L$, ΔV_{le} is the potential drop along the leader, and ΔV_{ce} is the potential drop generated by a uniform cylindrical space charge at the leader tip, which includes the direct components ΔV_{ce1} and the image charge component ΔV_{ce2} [20,21].

The following expressions may be derived in the case of leader development along the Z axis:

$$\Delta V_{le} = \int_H^{H+L} E_i(z)\,dz = E_i L, \tag{4}$$

$$\Delta V_{am} = \int_0^{H+L} E_0(z)\,dz = E_0(H+L) \quad \text{(in uniform atmospheric field)}, \tag{5}$$

$$\Delta V_{ce} = \Delta V_{ce1} + \Delta V_{ce2}, \tag{6}$$

$$\Delta V_{ce1} = \frac{q_{ce}L}{4\pi\varepsilon_0 a_{ce}^2(L+L_c)}\left[-\left(L^2+L_c^2\right) + a_{ce}^2 \ln\left[\frac{\sqrt{a_{ce}^2+L_c^2}+L_c}{\sqrt{a_{ce}^2+L^2}-L}\right] + L\sqrt{a_{ce}^2+L^2} + L_c\sqrt{a_{ce}^2+L_c^2}\right], \tag{7}$$

$$\Delta V_{ce2} = -\frac{q_{ce}L}{4\pi\varepsilon_0 a_{ce}^2(L+L_c)}\left[(2H+L)^2-(2H+2L+L_c)^2\right.$$
$$+a_{ce}^2\ln\left[\frac{\sqrt{a_{ce}^2+(2H+L)^2}-(2H+L)}{\sqrt{a_{ce}^2+(2H+2L+L_c)^2}-(2H+2L+L_c)}\right]$$
$$\left.+(2H+2L+L_c)\sqrt{a_{ce}^2+(2H+2L+L_c)^2}-(2H+L)\sqrt{a_{ce}^2+(2H+L)^2}\right]. \quad (8)$$

Eq. (3) can be split in three terms:

$$\Delta V = E_0 H + (E_0 - E_i)L - \Delta V_{ce}, \quad (9)$$

where the first term is associated with the initial potential for the leader development; the second corresponds to the potential increase due to the leader extension; the last term is due to the space charge which tends to reduce the available potential for the leader development. The simplified electrostatic model assumes that the propagation is stable if $\Delta V(L)$ remains positive and above a minimum value ΔV_c.

4.4.2. *Principle of the computation*

In order to calculate the potential difference ΔV as function of the leader length L, it is necessary to determine parameters L_c, a_{ce}, q_{ce} and E_i. It has been shown in previous studies that the axial field E_S in the space charge region of positive leaders is approximately constant with a value around 4.5 kV·cm^{-1} [1,7]: an upper limit value for L_c may be therefore obtained as:

$$L_c(m) = \frac{\Delta V}{E_S}. \quad (10)$$

The results derived from the Eq. (9) are consistent with observations from streak cameragrams of triggered lightning leaders [22] which indicate lengths L_c of the leader corona from a few meters up to 10 m. From the same optical data, the radius a_{ce} of the corona envelope was estimated between 0.5 and 2 m. The charge per unit length q_{ce} can be assumed to be equal to the minimum charge per unit length necessary to reproduce the thermal transition at the leader tip. Theoretical studies [7] give values around 50 µC·m^{-1} for positive leaders, consistent with the values measured under laboratory conditions [1,2]. For the internal field E_i, a value of a few kV·m^{-1} seems reasonable if most of the leader channel is thermalized.

The minimum potential for stable leader propagation, ΔV_c, calculated by using Eq. (9) and assuming a minimum corona length of 0.5 m, is equal to 225 kV. The flow chart of the computation of $\Delta V(L)$ is presented in Appendix B. Fig. 15 shows $\Delta V(L)$ computed for a structure of height $H = 50$ m and at various uniform ambient fields E_0. Two different patterns in variation of $\Delta V(L)$ can be recognized:

- at low values of ambient fields, $\Delta V(L)$ decreases below ΔVc, and the leader propagation is interrupted before the conditions for stabilization are reached;
- at higher values of ambient fields, $\Delta V(L)$ first decreases to a minimum and then starts to increase steadily. The minimum ambient field, at which this pattern develops, is called the 'stabilization field'. Its value for $H = 50$ m is 42 kV·m^{-1}.

4.4.3. *Influence of discharge parameters*

The simplified electrostatic approach described above enables us to understand the behavior of a positive leader-corona system. In particular, it allows us to get a clear picture of the influence of the different discharge parameters that are 'hidden' in the more complex self-consistent model. Similarly to the case in Fig. 15, calculations of the propagation curves has been made for several values of the corona width a_{ce}, the charge per unit length q_{ce} and the internal field E_i for a structure of height $H = 50$ m and an ambient field of $E_0 = 50$ kV·m^{-1} (Figs. 16–18).

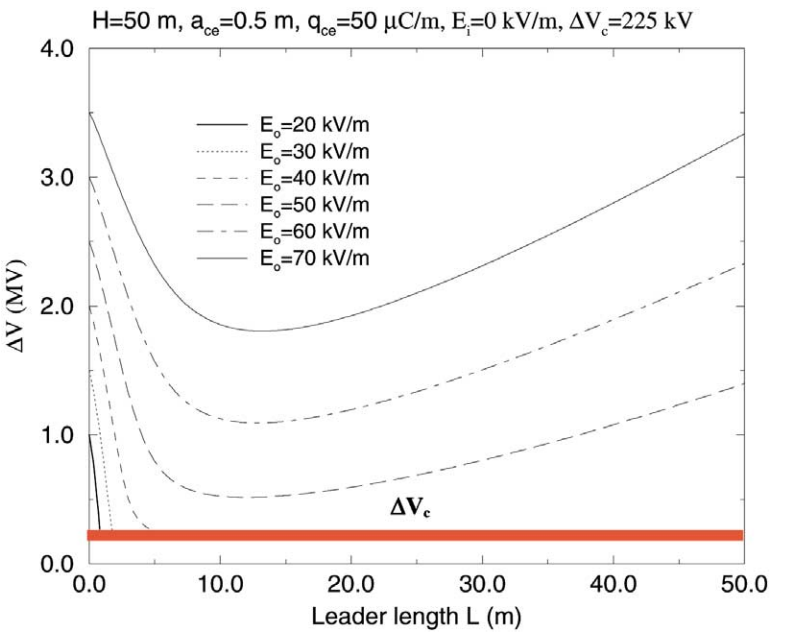

Figure 15. The potential difference at the leader tip, $\Delta V(L)$, as function of the leader length L for a rod of height $H = 50$ m and for different ambient fields E_0. The physical parameters used here are $L_c = 5$ m, $a_{ce} = 0.5$ m, $q_{ce} = 50\ \mu\text{C}\cdot\text{m}^{-1}$ and $E_i = 0\ \text{kV}\cdot\text{m}^{-1}$.

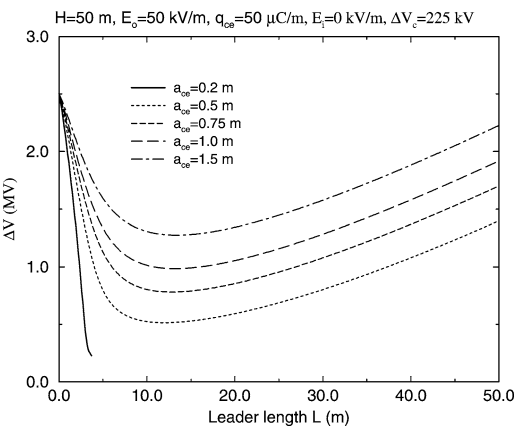

Figure 16. The same as in Fig. 15, but for the influence of corona width on the discharge propagation curves.

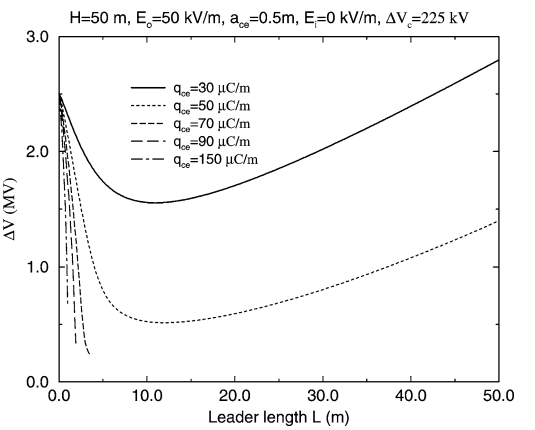

Figure 17. The same as in Fig. 15, but for the influence of the charge per unit length on the discharge propagation curves.

Figs. 16 and 17 illustrates the 'screening' effect of the space charge: for narrow corona envelopes and high charges per unit length, the leader does not reach conditions for a stable propagation. The increase of the internal field has similar influence, but its effect is limited for high atmospheric fields (Fig. 18). In all these cases, the leader extension is not enough to counterbalance the space charge which continuously reduces the available potential for the leader propagation.

The Fig. 19 shows the stabilization field computed for both positive and negative leaders using the physical model and the simplified electrostatic model. The leader parameters for the simplified model are chosen so that the calculated propagation curves fit the ones obtained with the physical model. The best parameters for the simplified model are for the positive discharge $q_{ce} = 50\ \mu\text{C}\cdot\text{m}^{-1}$, $a_{ce} = 0.5$ m, $E_s = 4.5\ \text{kV}\cdot\text{m}^{-1}$ and

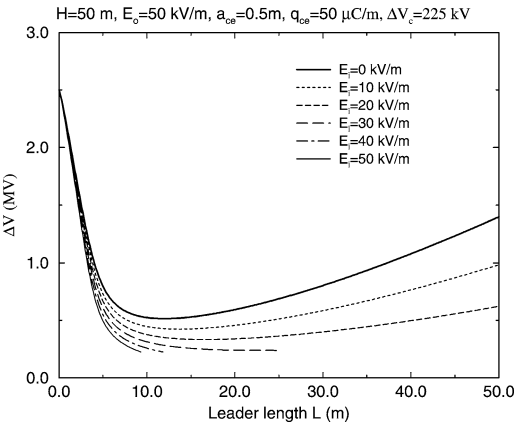

Figure 18. The same as in Fig. 15, but for the influence of the channel internal field on the discharge propagation curves.

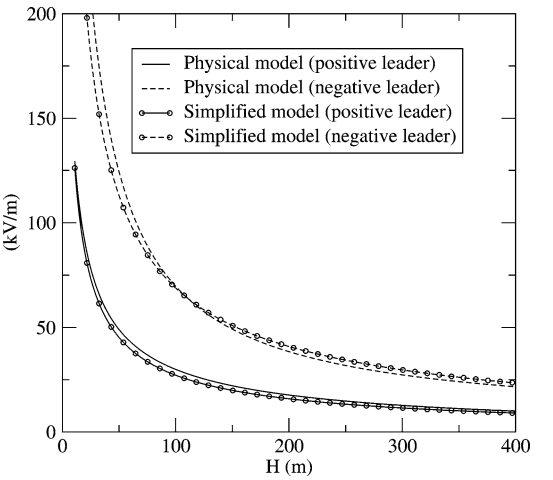

Figure 19. Comparison between the stabilization field computed with the physical model and the simplified electrostatic model. The parameters used for a positive leader are $q_{ce} = 50$ µC·m^{-1}, $a_{ce} = 0.5$ m, $E_s = 4.5$ kV·m^{-1}; for a negative discharge $q_{ce} = 140$ µC·m^{-1}, $a_{ce} = 0.5$ m, $E_s = 8$ kV·m^{-1}.

for a negative discharge $q_{ce} = 140$ µC·m^{-1}, $a_{ce} = 0.5$ m, $E_s = 8$ kV·m^{-1}. By using the previous parameters, this simplified electrostatic model can be used to simulate the development of a leader from a structure.

5. Conclusion

Comparison between laboratory and lightning leaders has shown that the lightning leader can propagate inside ambient electric field five times lower than the one needed in laboratory. This effect is mainly due to the value of the internal electric field along the leader. Numerical simulation of the leader channel behavior as a function of the current flowing through it shows that for low current (a few A) the internal electric field is mainly driven by electron-neutrals collisions and remains higher than 100 kV·m^{-1}. At larger currents associated with lightning leaders, thermal ionization dominates leading to a sharp decrease of the internal electric field down to a few kV·m^{-1}.

The ONERA/University of Padova discharge models have been adapted in both polarities to take into account the evolution of the internal electric field as a function of the current. These models have been used to simulate the inception and propagation of upward positive leaders triggered by the classical technique as well as the development of bi-directional leaders triggered in altitude.

These experimental and theoretical studies have demonstrated that upward leaders initiated from grounded structures can propagate in a stable or unstable regime according to the combined values of ambient electric field and height of the structure. For lightning protection purposes, the concept of stabilization field has been derived from the results of the proposed models. It has been defined as the minimum uniform ambient field which leads to a stable propagation of the leader starting for a given conducting object. Results of classical triggered lightning experiments have been used to validate this concept. Finally, a simplified electrostatic model has been proposed in order to clearly demonstrate the influence of discharge parameters (space charge radius, charge per unit leader length or internal leader field) on the leader propagation mode.

These models are already used within numerical tools for the design of lightning protection systems on aircraft and could be used in the future for the protection of ground structures.

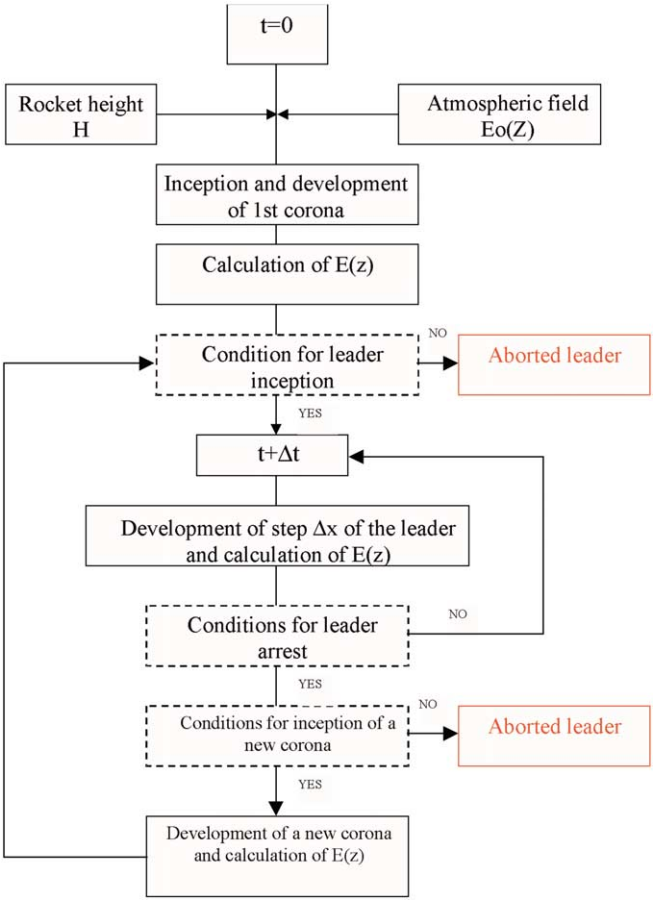

Figure 20. General flow-chart for the simulation of a leader in the model [4l]. Arrest conditions are related to insufficient E-field at the corona head or at the leader tip.

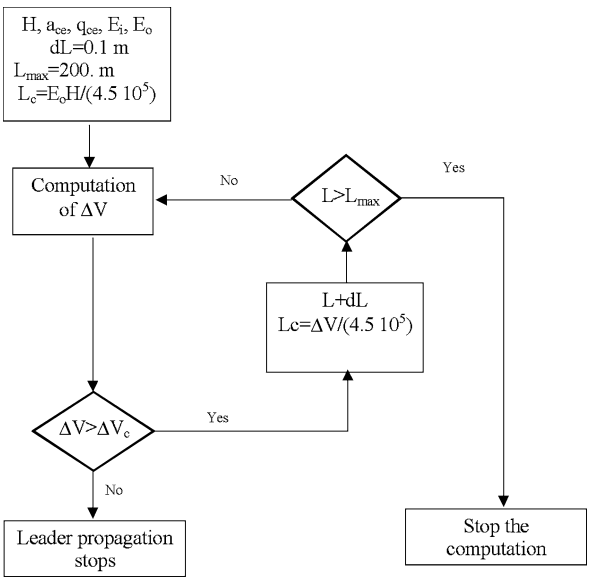

Figure 21. Flow chart of the computation of ΔV.

Appendix A

The main steps of the simulation code are given in the flow chart of Fig. 20 in the case of the simulation of a single leader. For the simulation of a bipolar system with 2 leaders of opposite polarities, as in the case of the altitude triggered flash, the general principles are similar, both developments being coupled through the evolution of the potential of the central conductor.

Appendix B

The flow chart of the electrostatic model is presented in Fig. 21. The input of the model is the ambient electric field E_0, the length H of the structure and the parameters a_{ce}, q_{ce}, E_i, ΔV_c associated with leader characteristics.

References

[1] Les Renardières Group, Long air gap discharges at Les Renardières – 1973 results, Electra 23 (1972) and Electra 35 (1974).
[2] Les Renardières Group, Positive discharges in long air gaps at Les Renardières – 1975 results and conclusions, Electra 53 (1977).
[3] Les Renardières Group, Negative discharges in long air gaps at Les Renardières – 1978 results, Electra 74 (1981).
[4] A. Bondiou, I. Gallimberti, Theoretical modelling of the development of positive sparks in long gaps, J. Phys. D 27 (1994).
[5] G.L. Bacchiega, A. Bondiou, I. Gallimberti, Theoretical modelling of the laboratory negative stepped leader, International Aerospace and Ground Conference On Lightning and Static Electricity (ICOLSE), May, 1994.
[6] I. Gallimberti, G. Bacchiega, A. Bondiou-Clergerie, P. Lalande, Fundamental processes in long air gap discharges, C. R. Physique 3 (2002) 1335–1359.
[7] I. Gallimberti, The mechanism of the long spark formation, J. Phys. Colloq. C 7 (7) (1979), C7-193.
[8] R.H. Golde, Lightning, Vol.1: Physics of Lightning, Academic Press, 1977.
[9] J.L. Boulay, Current waveforms observed during lightning strikes on aircraft, International Aerospace and Ground Conference on Lightning and Static Electricity (ICOLSE), NASA, Coco Beach, Floride, April 16–19, 1991.
[10] P. Laroche, A. Hubert, Eybert-Berard, Triggered flashes at TRIP 81. First results, AGU Fall Meeting, San Francisco, 1981, TP Onera n^o 1981–142.
[11] M.A. Uman, E.P. Krider, A review of natural lightning: experimental data and modelling, IEEE Trans. Electromag. Comp. EMC-24 (1982) 79–112.
[12] P. Laroche, V. Idone, A. Eybert-Berard, L. Barret, Observations of bi-directional leader development in a triggered lightning flash, International Aerospace and Ground Conference on Lightning and Static Electricity (ICOLSE), NASA, Coco Beach, Floride, April 16–19, 1991.
[13] P. Lalande, A. Bondiou-Clergerie, P. Laroche, A. Eybert-Berard, J.P. Berlandis, B. Bador, A. Bonamy, M.A. Uman, V. Rakov, Leader properties determined with triggered lightning techniques, J. Geophys. Res. 103 (D12) (1998) 14109.
[14] A. Castellani, A. Bondiou-Clergerie, P. Lalande, A. Bonamy, I. Gallimberti, Laboratory study of the bi-leader process from an electrically floating conductor. Part 1: General results, IEE Proc. Sci. 5 (1998) 185–192.
[15] A. Castellani, Calcul du champ électrique par la méthode des charges équivalentes pour la simulation d'une décharge bi-leader, Thèse de doctorat de l'Université Paris XI, Juin 1995.
[16] W.H. Press, B.P. Flannery, S.A. Teukolsky, W.T. Vetterling, Numerical Recipes, Cambridge.
[17] K. Berger, Development and properties of positive lightning flashes at Mount San Salvadore, Culham Conf. Section I2, 1975.
[18] J. Willett, D.A. Davis, P. Laroche, An experimental study of positive leaders initiating rocket-triggered lightning, Atmosph. Res. 51 (1999) 189–219.
[19] P. Lalande, A. Bondiou-Clergerie, P. Laroche, Determination of lightning strike zones on aircraft and helicopter. Results of the FULMEN program, Int. Conf. On Lightning and Static Electricity, Toulouse, June 1999.
[20] E. Durand, Electrostatique, Tome 1, Masson et C^{ie}, 1964.
[21] I. Gallimberti, M. Goldin, E. Poli, Field calculations for modelling long sparks, University of Padova, Upee – 82/07, May 1982.
[22] V. Idone, The luminous development of Florida triggered lightning, Res. Lett. Atmos. Electr. 12 (1992) 23–28.